Supplemental Material to "Fractional quantum Hall phases of bosons with tunable interactions: From the Laughlin liquid to a fractional Wigner crystal"

Tobias Graß,[1] Przemyslaw Bienias,[1] Michael J. Gullans,[2]
Rex Lundgren,[1] Joseph Maciejko,[3,4,5] and Alexey V. Gorshkov[1,6]

[1] *Joint Quantum Institute, NIST/University of Maryland, College Park, Maryland, 20742, USA*
[2] *Department of Physics, Princeton University, Princeton, New Jersey, 08544, USA*
[3] *Department of Physics, University of Alberta, Edmonton, Alberta T6G 2E1, Canada*
[4] *Theoretical Physics Institute, University of Alberta, Edmonton, Alberta T6G 2E1, Canada*
[5] *Canadian Institute for Advanced Research, Toronto, Ontario M5G 1Z8, Canada*
[6] *Joint Center for Quantum Information and Computer Science, NIST/University of Maryland, College Park, MD 20742, USA*

This Supplemental Material consists of three Sections. Sec. I extends the numerical study of the main text to other system sizes and torus ratios. Sec. II provides characteristic energy spectra of each phase. In Sec. III, we have computed the entanglement entropy in the Laughlin liquid phase and in the fractional Wigner crystal phase.

I. DEPENDENCE OF NUMERICAL RESULTS ON SYSTEM SIZE AND/OR GEOMETRY

Most of our numerical data presented in the main text was for $N = 8$ bosons, on a torus with axes ratio $a/b = 0.9$. For incompressible phases, system size and geometry tend to play only a minor role. This is no longer true when the system becomes compressible. In this section of the Supplemental Material, we present some additional data obtained by varying the axis ratio of the torus, and by considering systems of $N = 9$ and $N = 10$ bosons.

A. Phase diagram

First, we consider the phase diagram on a strongly squeezed torus with axis ratio $a/b = 0.5$. Here, we have restricted our study to fully repulsive interactions, $u_2, u_4 > 0$. Again the direct gap at $\mathbf{K} = (0, 0)$ serves as an indicator of phase boundaries. We plot the gap for $N = 8$, as shown in Fig. S1 (a). The data now suggests the existence of an additional phase. By evaluating the ground-state pair correlation functions, we identify the different phases. As before, we find the Laughlin liquid, and the bubble phases B1 and B2, which are now separated by an intermediate phase B3 consisting of three stripes, see Fig. S1 (c). Moreover, it turns out that the FWC is strongly deformed, and does not exhibit N_ϕ separate peaks anymore, see Fig. S1 (b). In terms of overlap, this region is still smoothly connected to the Laughlin state.

Next, we compare the phase diagram obtained for $N = 8$ bosons with the one for $N = 9$, while keeping the geometry unchanged ($a/b = 0.9$). We find all the phases which were present also for $N = 8$ (Laughlin liquid, FWC, bubbles B1 and B2), plus an additional phase consisting of three stripes. The pair-correlation function for this phase is shown Fig. S2 (b). In the phase diagram of Fig. S2 (a), the stripe phase occurs at intermediate values of u_2, and small values of u_4. Such a phase has also been seen before in a system of dipolar atoms [1]. Apart from this intermediate stripe phase, the phase diagrams at $N = 8$ and $N = 9$ are qualitatively the same.

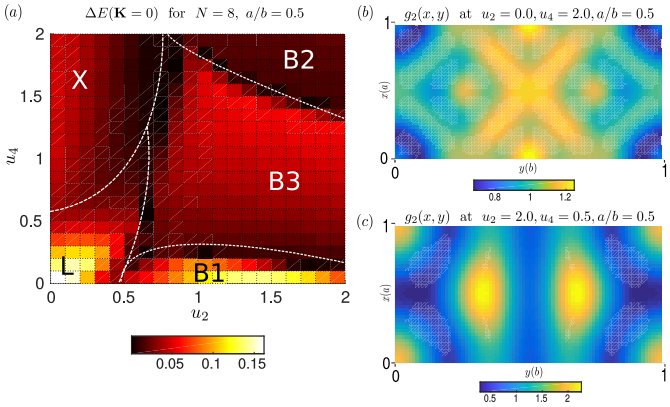

FIG. S1. (a) By plotting the direct energy gap at $\mathbf{K} = 0$, we draw a phase diagram in the parameter space given by repulsive u_2 and u_4. As in the main text, our data was obtained for $N = 8$ bosons, but now the torus is squeezed to an axis ratio $a/b = 0.5$. As for the less anisotropic case shown in the main text, this squeezed torus also hosts the Laughlin phase (L), and the bubble phases B1 and B2, but now a third bubble phase B3 lies in between those two regimes. The FWC crystal has been deformed, as shown in the pair-correlation function in panel (b). We thus denote this phase by an X. Panel (c) shows the pair-correlation function of the B3 phase, consisting of three bubbles.

B. Fractional Wigner crystal

The symmetry-breaking in the FWC phase has a characteristic two-fold ground state degeneracy at $\mathbf{K} = 0$. Thus, to study the robustness of this phase upon changes in the geometry, we may just track the lowest eigenenergies at $\mathbf{K} = 0$ as a function of the axis ratio a/b. This data, for system sizes $N = 8, 9, 10$ is shown in Fig. S3.

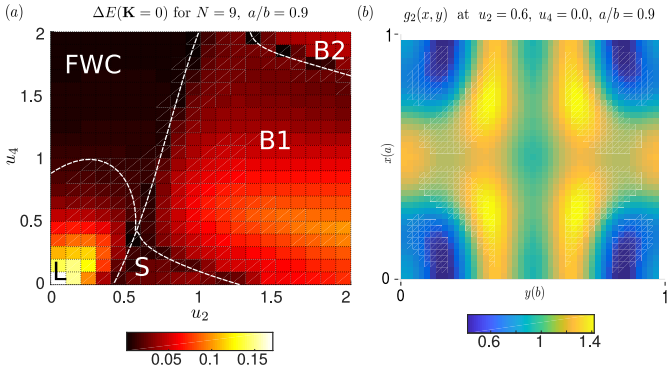

FIG. S2. (a) By plotting the direct energy gap at $\mathbf{K} = 0$, we draw a phase diagram in the parameter space given by repulsive u_2 and u_4. Here we use the same axis ratio as in the main text ($a/b = 0.9$), but increase the system size to $N = 9$ bosons and $N_\phi = 18$ fluxes. We find a similar phase diagram, hosting the Laughlin phase (L), the fractional Wigner crystal phase (FWC), the bubble phases B1 and B2, plus an additional phase S at intermediate values of u_2. (b) By evaluating the ground state pair-correlation function, we identify the intermediate phase S as a phase consisting of three stripes along the x-axis.

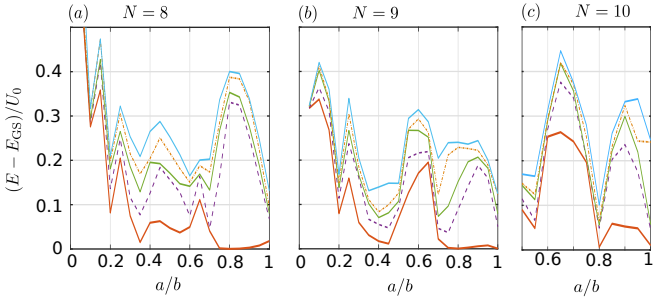

FIG. S3. For different system sizes $N = 8, 9, 10$, we plot the energies of the five lowest excitations at $\mathbf{K} = 0$, relative to the ground state energy, as a function of the axis ratio a/b. Thus, the red lines correspond to the direct gap which, due to the two-fold degeneracy, vanishes in the FWC phase. The degenerate regime extends from the isotropic torus ($a/b = 1$), to values about $a/b = 0.8$. All data was obtained at $u_2 = 0$ and $u_4 = 2.0$.

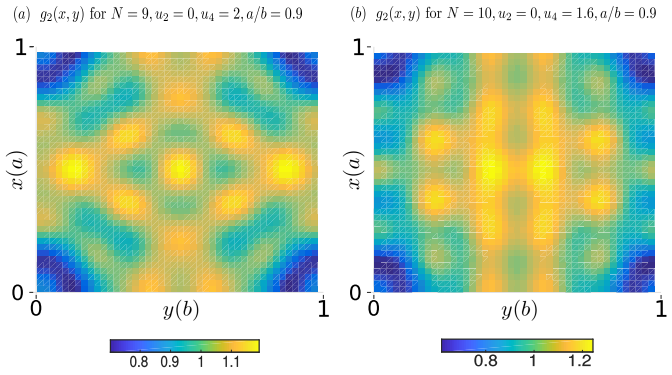

FIG. S4. We plot, for $N = 9$ (a) and $N = 10$ (b), the ground state pair-correlation function in the FWC phase. The number of peaks (+origin) is equal to $2N$.

We note that, even in the FWC phase, the ground state degeneracy is slightly lifted at $N = 10$, but this lifting is sufficiently small to identify a quasi-degenerate regime. With this, the characteristic degeneracy is found to extend from the isotropic limit $a/b = 1$ down to squeezed ratios $a/b \approx 0.8$.

For larger deviations from the isotropic case, the correlation function does not exhibit N_ϕ separate peaks anymore, as shown in Fig. S1(b). The question arises whether such a geometry dependence would also occur in a large system on a flat plane? Due to the non-liquid behavior of the phase, finite-size effects play an important role for choosing the energetically most favorable arrangement. Squeezing the torus enhances finite-size effects, as one axis becomes very short. We therefore believe that the phases obtained near $a/b = 1$ are most likely the ones which will be seen in a thermodynamically large system.

By plotting the pair-correlation function of the ground state within the two-fold degenerate regime, we verify that the state exhibits fractional crystal order for different system sizes ($N = 9$ and $N = 10$). As seen in Fig. S4, the number of peaks plus the origin (i.e. the position of the probe particle), is given by $2N$, that is, we always get a half-filled lattice.

II. ENERGY SPECTRA IN DIFFERENT PHASES

In Fig. 2 of the main text, we have plotted ground state pair correlation functions in order to identify the symmetry-broken order. Each phase can also be characterized by its energy spectra which, for the same parameters as in Fig. 2 of the main text, are plotted in Fig. S5.

III. ENTANGLEMENT ENTROPY IN THE FRACTIONAL WIGNER CRYSTAL

Different quantities have proven useful for classifying topologically ordered system, including ground state degeneracies on the torus, the number of edge states in systems with open boundaries, or the topological entropy. In the main text, we have discussed the ground state degeneracies of the fractional Wigner phase. In particular, we have argued that these degeneracies are geometrical (i.e. understood from the symmetry breaking order), apart from the trivial two-fold topological degeneracy of a toroidal system at half filling. This observation excludes non-Abelian phases.

In this Supplemental Material, we discuss a topological quantum number provided by the von Neumann entropy of entanglement $S(L)$. The entropy is expected to scale linearly with the boundary L of a bi-partite cut through the system, and in topological systems, it is non-zero in the limit $L \to 0$. Its value, known as "topological en-

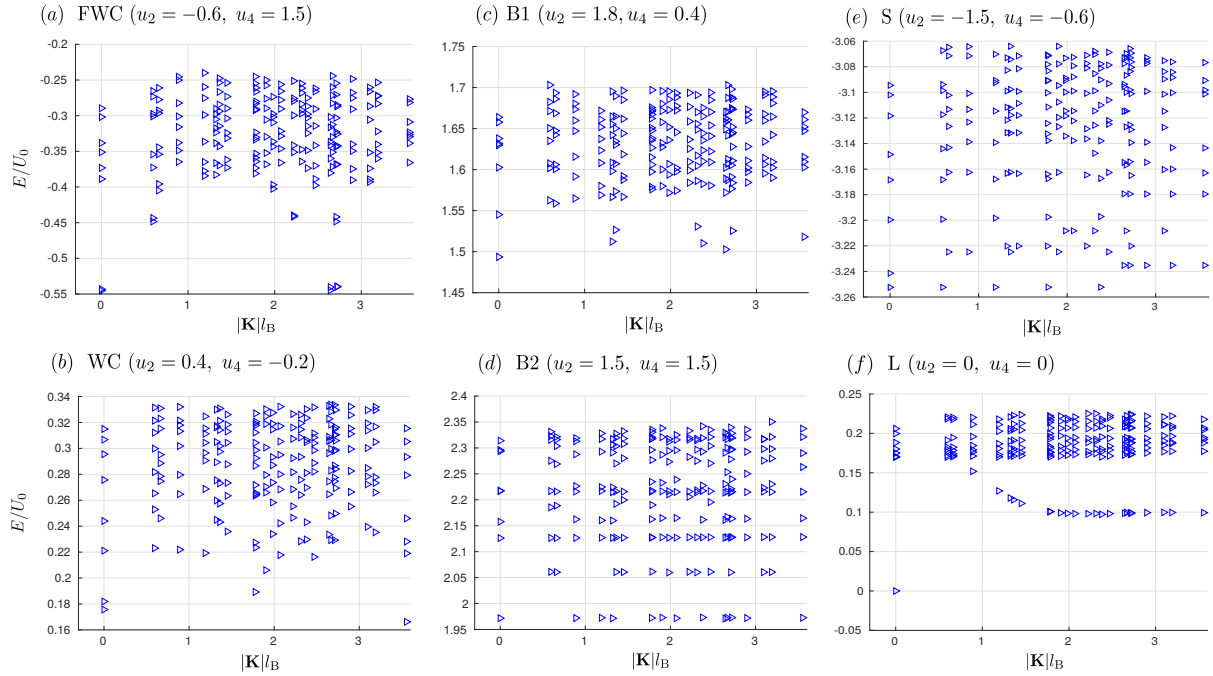

FIG. S5. For the same parameters u_2, u_4 as used in Fig. 2 of the main text, we plot the energy spectra ($N = 8, a/b = 0.9$). Pseudomomenta $|\mathbf{K}|$ are in units of the inverse magnetic length $l_\mathrm{B} \equiv \sqrt{2\pi N_\phi/(ab)}$.

tropy", measures the quantum dimension of a topological field theory [2, 3].

We evaluate the entanglement entropy by making two orbital cuts, which in the Landau gauge are roughly equivalent to spatial cuts along the translational invariant direction. In this way, we divide the torus into two equal cylinders, each with two boundaries of size L, given by the circumference in this direction (i.e. by b). This length can continuously be tuned via the aspect ratio of the torus, providing a numerically feasible way of determining the topological entropy [4].

In Fig. S6, we have calculated the entanglement entropy in a system of 8 bosons. We have used this data to extrapolate the topological entropy. For a "pure" Laughlin state (i.e. for ground state of the parent Hamiltonian $u_2 = u_4 = 0$), the topological entropy is obtained with moderate accuracy: $\gamma = 0.4315 \pm 0.0010$, which is is off by about 30% from the theoretical expected value $\gamma = \log(\sqrt{m})$ for a Laughlin state at filling $\nu = 1/m$. However, the entropy is dramatically modified even by small non-zero values of higher pseudopotentials: For $u_4 = 0.3$, which we believe to be still in the Laughlin liquid phase, a linear scaling of the entanglement entropy is observed only within a subset of points, and the extrapolated value for the topological entropy increases to $\gamma = 1.50 \pm 0.07$. Upon further increasing u_4, the regime of linear scaling further decreases. If we nevertheless attempt to extract a topological entropy, our estimate within the fractional Wigner phase is about $\gamma = 2.1 \pm 0.1$. In view of these extremely large numbers, we believe that these results are strongly influenced by finite-size effects.

The breaking of translational symmetry makes it particularly difficult to extract the topological entropy with high accuracy, since tuning the aspect ratio of the torus triggers transitions between different crystal structures, seen also in the energy spectra shown in Fig. S3. The range of parameters which can be used to extrapolate the topological entropy is therefore restricted to relatively small intervals. In contrast, in the liquid phase such transitions are absent, and much more data points become available.

[1] N. R. Cooper, E. H. Rezayi, and S. H. Simon, Phys. Rev. Lett. **95**, 200402 (2005).
[2] A. Kitaev and J. Preskill, Phys. Rev. Lett. **96**, 110404 (2006).
[3] M. Levin and X.-G. Wen, Phys. Rev. Lett. **96**, 110405 (2006).
[4] A. M. Läuchli, E. J. Bergholtz, and M. Haque, New J. Phys. **12**, 75004 (2010).

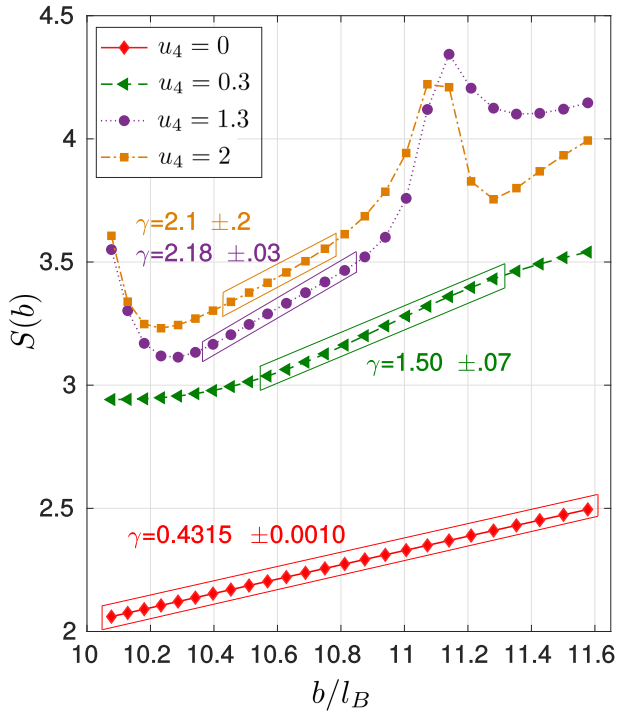

FIG. S6. We plot the entanglement entropy of $N = 8$ bosons at filling $\nu = 1/2$, as obtained by an orbital cut of the torus into two halves. All curves are for $u_2 = 0$, with different values of u_4. The entropy is ploted as a function of the length b along y-direction, which parametrizes the boundary size between the two subsystems. The length is determined by the aspect ratio ξ, $b = \sqrt{2\pi N_\Phi/\xi}$, and the data point in the figure are obtained by varying ξ from 0.99 (points on the left) to 0.75 (points on the right). The data points marked by the boxes have been used to extrapolate the topological entropy $\gamma = -S(0)/2$.